Supporting Information

Thermal and Bisphenol-A Adsorption Properties of Zinc Ferrite/*β*-Cyclodextrin Polymer Nanocomposite

Ruksana Sirach[1], Pragnesh N Dave[*,1]

[1]*Department of Chemistry, Sardar Patel University, Vallabh Vidyanagar, 388 120, Gujarat, India*

*Corresponding author: *pragnesh7@yahoo.com*

Table

Table S1. Details of chemicals used in the present study (purity ~98-99%)

Table S2. Temperature at different conversion percentage values for the decomposition of *β*-CD-E-T and *β*-CD-E-T/$ZnFe_2O_4$ (*β*=5, 10, 15, and 20 ºC min^{-1})

Figures

Fig. S1 Calibration curve of BPA

Fig. S2 BJH analysis for the pore size distribution and N_2 adsorption-desorption curve (Inset) of *β*-CD-E-T/$ZnFe_2O_4$.

Fig. S3 Conversion plots ($\alpha \rightarrow T$) of (a) *β*-CD-E-T and *β*-CD-E-T/$ZnFe_2O_4$ at 5, 10, 15, and 20 $^oC\ min^{-1}$

Fig. S4 Kinetics plots of *β*-CD-E-T (a) FWO, (b) KAS, and *β*-CD-E-T/$ZnFe_2O_4$ (c) FWO, and (d) KAS

Fig. S5 Average activation energy of *β*-CD-E-T and *β*-CD-E-T/$ZnFe_2O_4$ obtained using FWO, KAS, it-FWO, and it-KAS method.

Fig. S6 Effect of (a) *β*-CD-E-T/$ZnFe_2O_4$ dose and (b) BPA amount in aqueous solution on the adsorption capacity and R% of *β*-CD-E-T/$ZnFe_2O_4$

Fig. S7 Plot of ln K_e against 1/*T* for the removal of BPA using *β*-CD-E-T/$ZnFe_2O_4$ adsorbent

Equations

Linear forms of Langmuir equation:

$$\frac{C_e}{q_e} = \frac{1}{q_m} C_e + \frac{1}{K_L q_m} \quad \text{(S1)}$$

$$\frac{q_e}{C_e} = K_L q_m - K_L q_e \quad \text{(S2)}$$

$$\frac{1}{q_e} = \frac{1}{q_m} + \frac{1}{K_L q_m} \times \frac{1}{C_e} \quad \text{(S3)}$$

$$q_e = q_m - \frac{1}{K_L} \times \frac{q_e}{C_e} \quad \text{(S4)}$$

The plot of C_e/q_e vs. C_e (Eq. S1), q_e/C_e vs. q_e (Eq. S2), $1/q_e$ vs. $1/C_e$ (Eq. 3), or q_e vs. q_e/C_e can be used to obtain Langmuir isotherms parameters using slope and the interception.

Tables

Table S1. Details of chemicals used in the present study (purity ~98-99%)

Chemical	**Molar mass (g mol^{-1})**	**CAS**	**Supplier**
Zinc (II) nitrate hexahydrate	297.5	10196-18-6	SRL
Iron (III) nitrate nonahydrate	404.0	7782-61-8	SRL
sodium hydroxide	40.0	1310-73-2	Samir Tech
Sodium acetate	82.0	127-09-3	SRL
β-Cyclodextrin	1135.0	7585-39-9	HiMedia
Epichlorohydrin	92.5	106-89-8	Merck
Tetrafluoroterephthalonitrile	200.1	1835-49-0	Merck
Ethylene diamine	60.1	107-15-3	SRL
Tetrahydrofuran	72.1	109-99-9	Samir Tech
Ethylene glycol	62.1	107-21-1	SRL
Bisphenol A	228.3	80-05-7	SRL

Table S2. Temperature at different conversion percentage values for the decomposition of *β*-CD-E-T and *β*-CD-E-T/$ZnFe_2O_4$ (*β*=5, 10, 15, and 20 ºC min^{-1})

	β-CD-E-T				*β*-CD-E-T/$ZnFe_2O_4$			
Extent of conversion α (%)	Temperature (K) at different heating rates				Temperature (K) at different heating rates			
	T_α (5)	T_α (10)	T_α (15)	T_α (20)	T_α (5)	T_α (10)	T_α (15)	T_α (20)
10	567	580	587	594	561	572	577	580
12.5	573	585	592	599	566	577	582	585
15	577	589	596	602	570	581	586	590

17.5	581	592	599	606	573	585	589	593
20	584	595	602	608	576	588	592	597
22.5	586	598	605	611	579	591	595	599
25	589	600	607	613	581	593	598	602
27.5	591	602	609	615	584	596	600	604
30	593	604	611	617	586	598	602	607
32.5	594	606	612	618	588	600	604	609
35	596	608	614	620	590	602	606	611
37.5	597	609	616	622	592	603	608	612
40	599	611	617	623	593	605	610	614
42.5	600	612	619	625	595	607	612	616
45	602	614	620	626	597	609	613	618
47.5	603	615	622	627	598	610	615	619
50	604	617	623	629	600	612	616	621
52.5	605	618	624	630	602	613	618	622
55	607	620	626	631	603	615	620	624
57.5	608	621	627	632	605	617	621	626
60	609	622	628	634	607	618	623	627
62.5	611	624	630	635	609	620	625	629
65	612	625	631	636	610	622	626	630
67.5	614	627	633	638	612	623	628	632
70	616	629	634	639	614	625	630	634
72.5	618	631	636	641	616	627	632	636
75	620	632	638	642	619	629	634	638
77.5	622	635	639	644	622	632	636	640
80	625	637	642	646	625	635	639	642
82.5	628	640	644	648	629	638	642	645
85	631	643	647	651	633	642	645	648
87.5	636	647	651	654	639	647	649	652
90	641	653	656	658	647	653	655	657

Figures

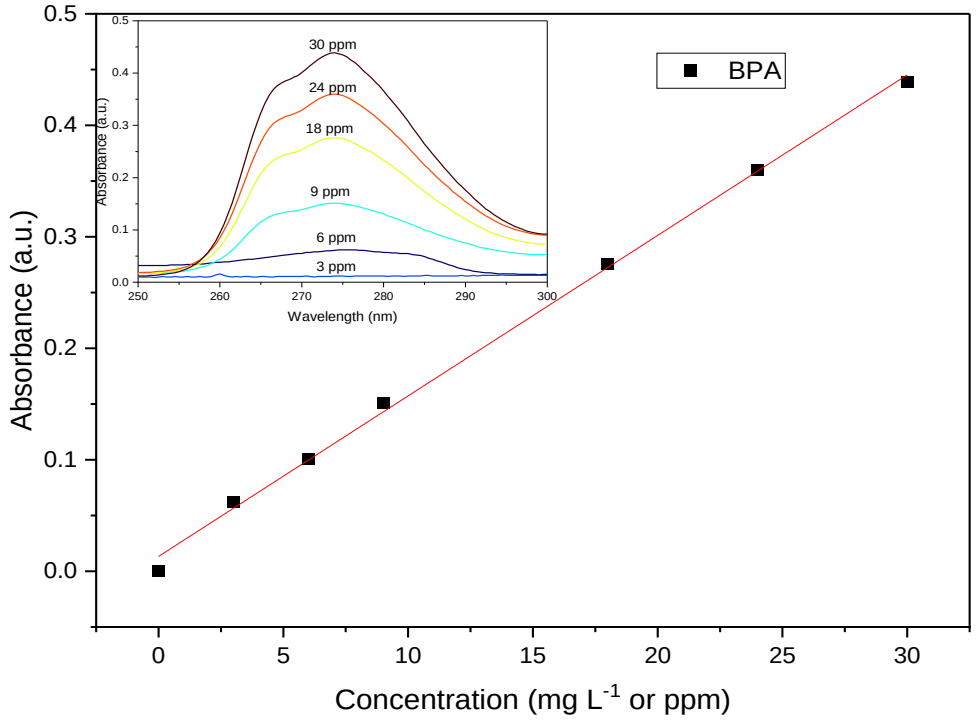

Fig. S1 Calibration curve of BPA

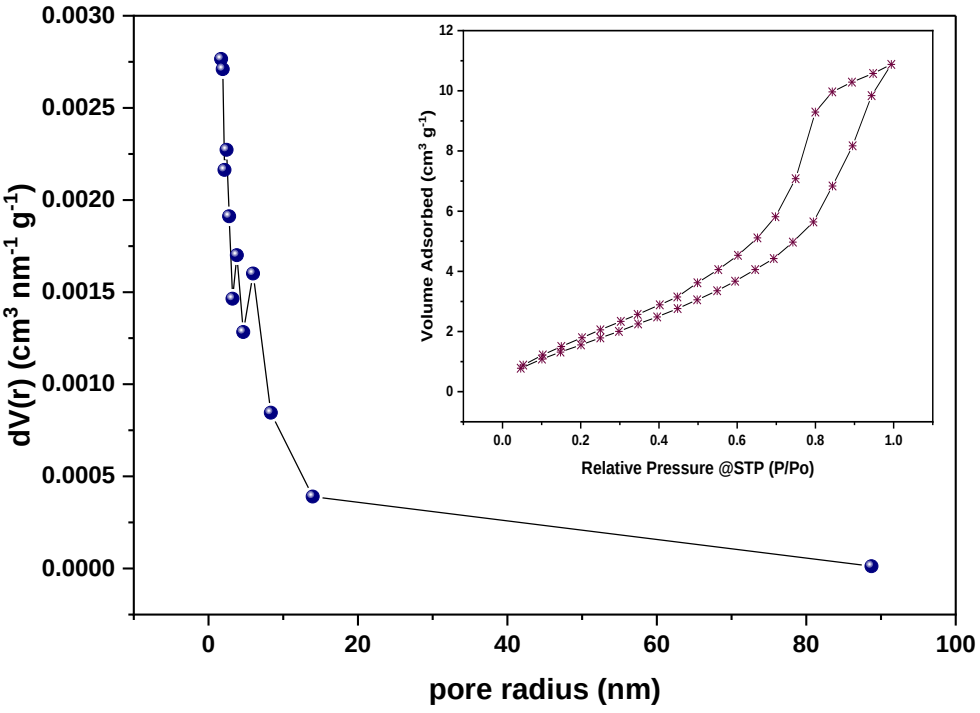

Fig. S2 BJH analysis for the pore size distribution and N_2 adsorption-desorption curve (Inset) of β-CD-E-T/$ZnFe_2O_4$

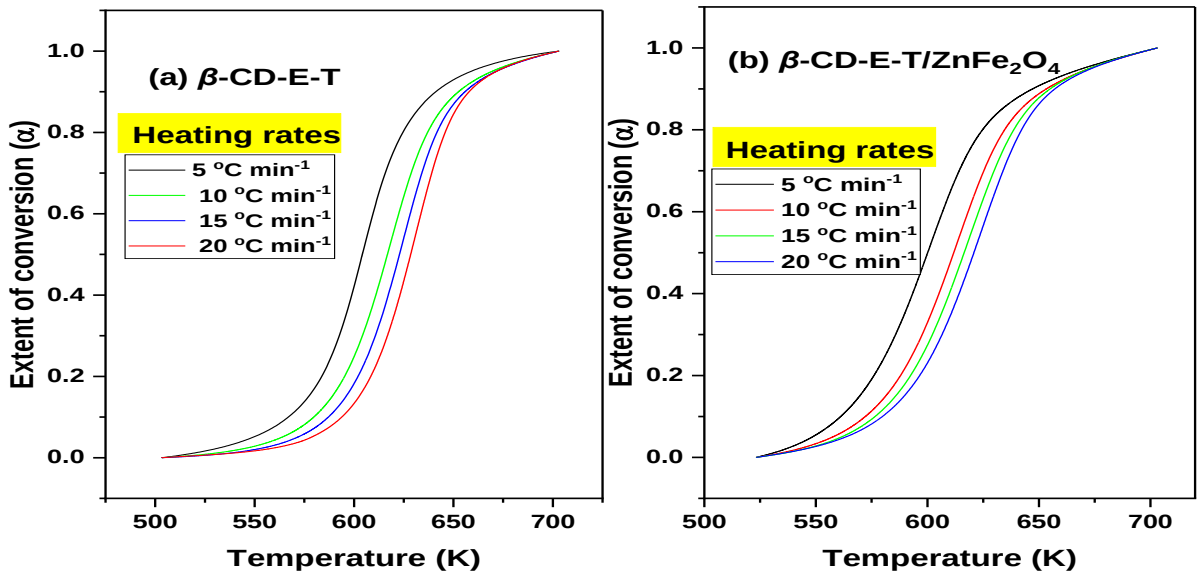

Fig. S3 Conversion plots ($\alpha \rightarrow T$) of (a) β-CD-E-T and β-CD-E-T/$ZnFe_2O_4$ at 5, 10, 15, and 20 $^oC\ min^{-1}$

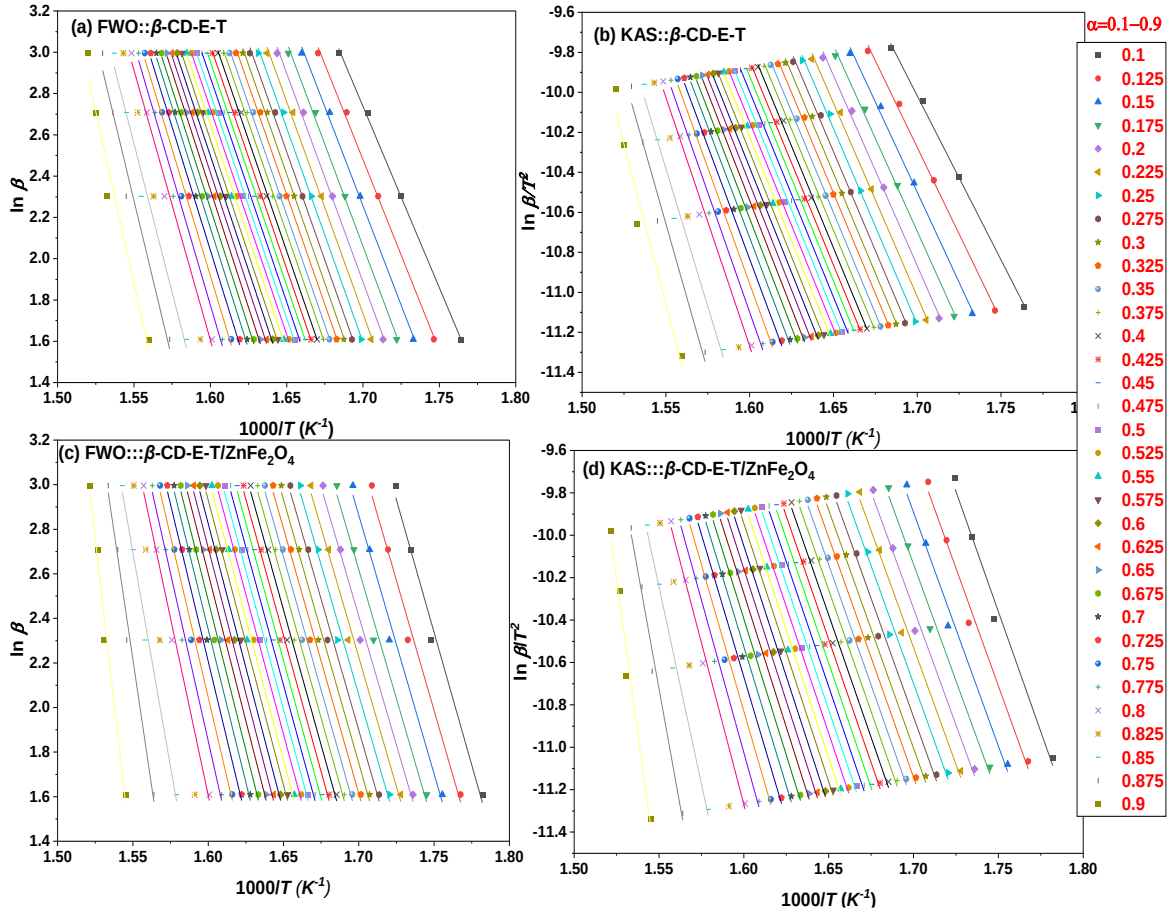

Fig. S4 Kinetics plots of β-CD-E-T (a) FWO, (b) KAS, and β-CD-E-T/$ZnFe_2O_4$ (c) FWO, and (d) KAS

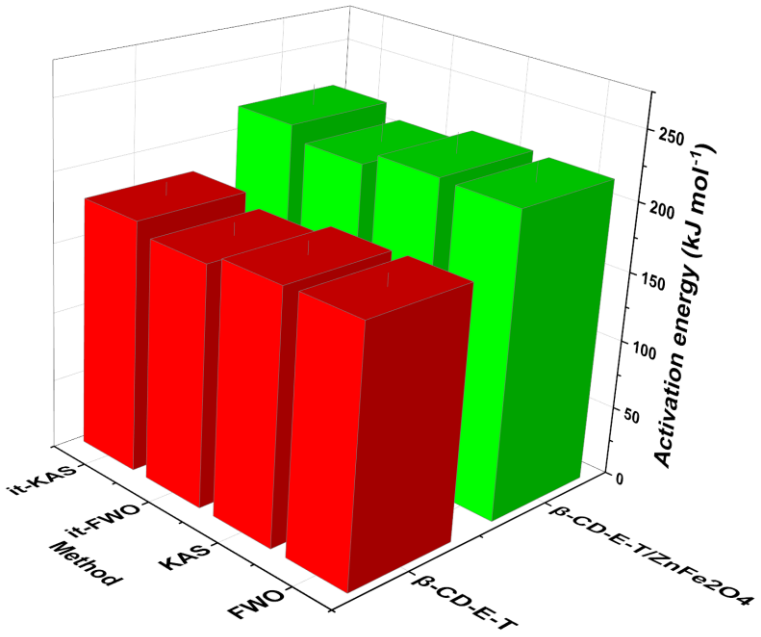

Fig. S5 Average activation energy of β-CD-E-T and β-CD-E-T/$ZnFe_2O_4$ obtained using FWO, KAS, it-FWO, and it-KAS method.

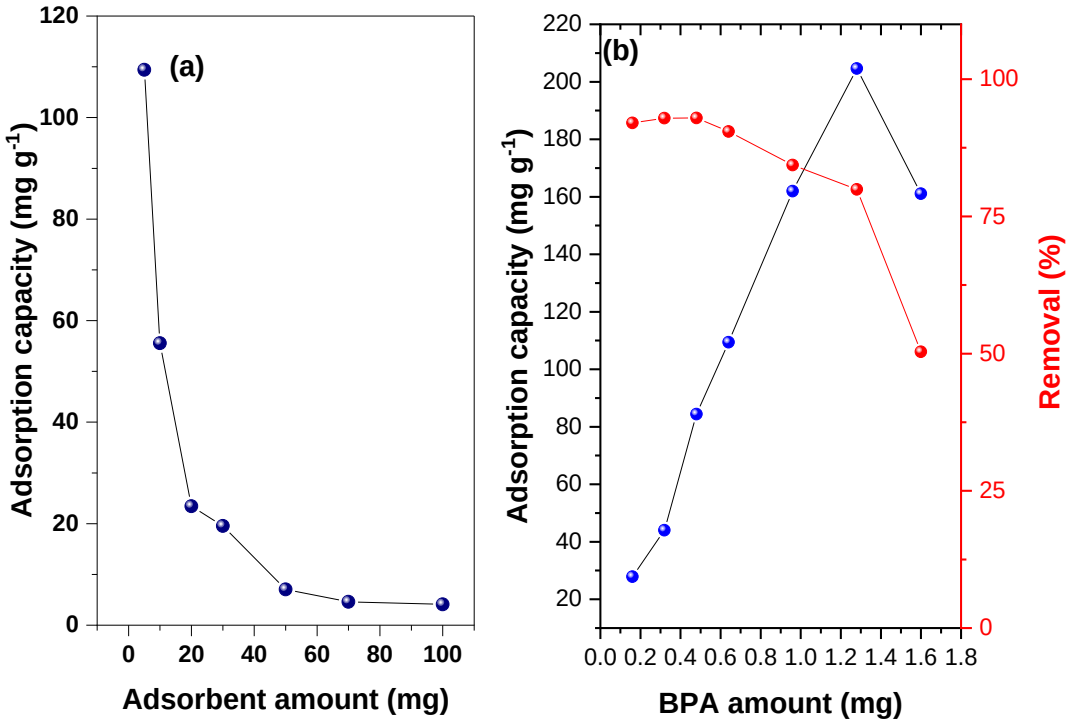

Fig. S6 Effect of (a) β-CD-E-T/$ZnFe_2O_4$ dose and (b) BPA amount in aqueous solution on the adsorption capacity and R% of β-CD-E-T/$ZnFe_2O_4$

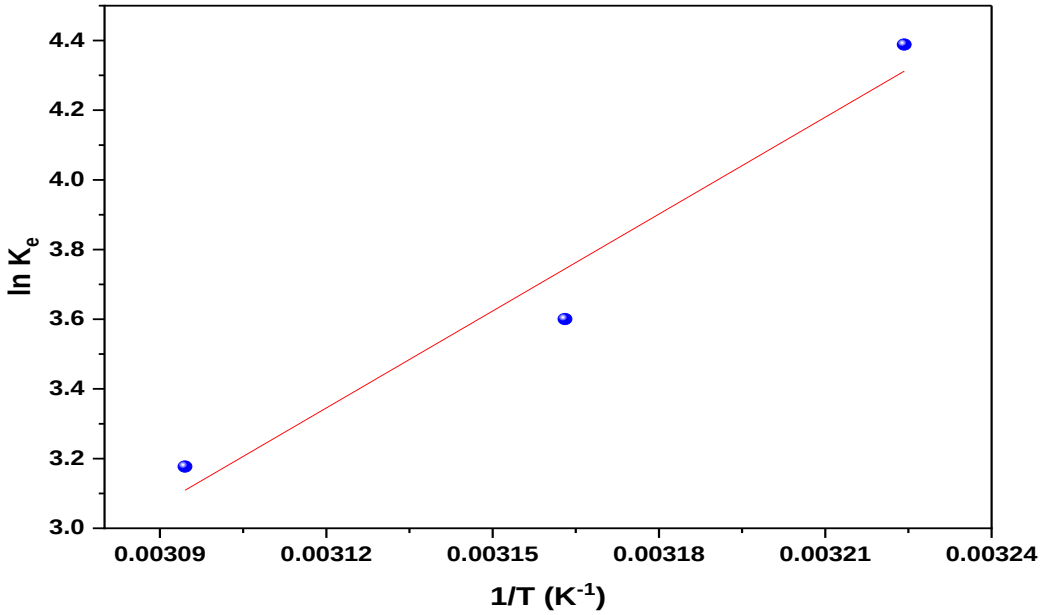

Fig. S7 Plot of ln K_e against 1/T for the removal of BPA using β-CD-E-T/$ZnFe_2O_4$ adsorbent